Three-Dimensional Optical Pulse Simulation Using the FDTD Method

Dennis Sullivan, *Senior Member, IEEE*, Jun Liu, and Mark Kuzyk

***Abstract*—As the use of optical waveguides expands, it would be desirable to have an explicit three-dimensional simulation method to analyze characteristics and develop new devices. One such method is the finite-difference time-domain (FDTD) method. The FDTD method requires a relatively high sampling density per wavelength, making simulation over distances of several wavelengths difficult. Several techniques are described to make such a simulation possible with limited computer resources. Among them is a moving problem space, which holds the pulse in the middle and moves the background medium past the pulse. Simultaneously, Fourier and wavelet analyses are used to characterize the pulse.**

***Index Terms*—Nonlinear, optical fiber, simulation.**

I. Introduction

ONE OF THE most widely used methods of electromagnetic (EM) simulation is the finite-difference time-domain (FDTD) method [1]. Its strength lies largely in its explicit nature: an implementation of the time-domain Maxwell's equations, which makes no approximations other than the finite differencing of the spatial and temporal derivatives. However, this explicit nature is a drawback in simulating EM phenomena at the high frequencies of light. FDTD requires many points per wavelength, and the small wavelengths of light dictate a very dense sampling rate. This becomes particularly difficult in three dimensions [2], [3].

This paper describes techniques by which FDTD can be used to simulate pulse propagation over relatively large distances. This could be of use in the simulation of numerous different optical waveguides or other devices. However, we will focus on the simulation of nonlinear optical fibers to demonstrate these methods.

It is expected that computer simulation can contribute significantly to the development of devices based on nonlinear optical fibers primarily for two reasons: 1) there is a greater need for explicit understanding of the nonlinear EM phenomena, particularly the phase information and 2) extremely complex physical models can be simulated and easily altered. This is an enormous advantage over fabricating experimental models.

Manuscript received April 8, 1999. This work was supported by the Army Research Office under Grant DAAH04-96-1-0406, by the Air Force Office of Scientific Research, by the San Diego Supercomputer Center under a grant, and by the Information Technology Program of NASA under a grant.

D. Sullivan is with the Department of Electrical Engineering, University of Idaho, Moscow, 83844-1023 USA (e-mail: dennis@ee.uidaho.edu).

J. Liu is with Maxim Integrated, Portland, OR 97701 USA.

M. Kuzyk is with the Materials Science Program, Physics Department, Washington State University, Pullman, WA 99164-2814 USA (e-mail: mark_kuzyk@wsu.edu).

Publisher Item Identifier S 0018-9480(00)05465-X.

The FDTD method has been shown to be capable of simulating dispersive and nonlinear EM phenomena of the type found in optical fibers [4], [5]. Such simulations have been carried out by several research groups, but three-dimensional simulation is problematic because of the computer resources required. The FDTD method requires from 10 to 30 points per wavelength. Wavelengths in optical fibers tend to be on the order of a micrometer, thus, simulation of more than a few micrometers become unwieldy when all three dimensions are involved.

In this paper, a different approach to the simulation of optical-fiber propagation is described: the propagating pulse is held in the middle of the problem space. In effect, the frame of reference of the simulation is moving with the propagating pulse. Propagation over relatively long distances can be simulated using a limited amount of computer resources.

Since the frame of reference is moving, methods are needed to quantify the changes to the pulse as it is propagating. A fast wavelet transform is used to record the changes to the shape of the pulse. This reduces the pulse to a small group of parameters that can be used to resynthesize the pulse at a later time. However, another method is needed to quantify macroscopic parameters, such as the speed of the pulse and its attenuation as it propagates. This is accomplished by a running Fourier transform operating at the center frequency of the pulse.

Section II of this paper briefly reviews the FDTD method with emphasis on how it handles nonlinear and dispersive material. Section III describes things that are necessary to make three-dimensional simulation a tractable problem. Besides the moving problem space, oblong cells are used to maximize resolution in the propagation direction and reduce the number of points in the transverse direction. Furthermore, the symmetry of single-mode fibers is exploited to reduce the problem space by one-fourth. Section IV describes the analysis methods and how they are implemented in the moving problem space. Two examples are given that illustrate these methods: one of propagation in dispersive media and one of propagation in nonlinear media. In Section V, we demonstrate the flexibility of the method by simulating the transition of a pulse from a linear to a nonlinear fiber.

II. FDTD Method

The FDTD method implements the time-domain Maxwell's equations [6]

$$\frac{\partial \boldsymbol{D}(\boldsymbol{x}, t)}{\partial t} = \frac{1}{\sqrt{\varepsilon_0 \mu_0}} \cdot \nabla \times \boldsymbol{H}(\boldsymbol{x}, t) \tag{1a}$$

and

$$\boldsymbol{D}(\boldsymbol{x}, t) = \varepsilon_r \cdot \boldsymbol{E}(\boldsymbol{x}, t) + \boldsymbol{P}_L(\boldsymbol{x}, t) + \boldsymbol{P}_{\mathrm{NL}}(\boldsymbol{x}, t) \tag{1b}$$

$$\frac{\partial \boldsymbol{H}(\boldsymbol{x}, t)}{\partial t} = -\frac{1}{\sqrt{\varepsilon_0 \mu_0}} \nabla \times \boldsymbol{E}(\boldsymbol{x}, t). \tag{1c}$$

(The above uses normalized units [7].) Starting with two of the individual equations described by the vectors in (1a) and (1c), the difference equations can be developed as follows:

$$\begin{aligned} &D_z^{n+1/2}(i, j, k+1/2) \\ &\quad = D_z^{n-1/2}(i, j, k+1/2) + \frac{\Delta T}{\Delta x \cdot \sqrt{\varepsilon_0 \mu_0}} \\ &\qquad \cdot \Big(H_y^n(i+1/2, j, k+1/2) - H_y^n(i-1/2, j, k+1/2) \\ &\qquad\quad - H_x^n(i, j+1/2, k+1/2) + H_x^n(i, j-1/2, k+1/2) \Big) \end{aligned} \tag{2a}$$

$$\begin{aligned} &H_z^{n+1}(i+1/2, j+1/2, k) \\ &\quad = H_z^n(i+1/2, j+1/2, k) + \frac{\Delta T}{\Delta x \cdot \sqrt{\varepsilon_0 \mu_0}} \\ &\qquad \cdot \Big(E_y^{n+1/2}(i+1, j+1/2, k) - E_y^{n+1/2}(i, j+1/2, k) \\ &\qquad\quad - E_x^{n+1/2}(i+1/2, j+1, k) + E_x^{n+1/2}(i+1/2, j, k) \Big) \end{aligned} \tag{2b}$$

where Δx is the cell size and ΔT is the time interval between iterations. The position vector x has been replaced by the position parameters i, j, k, in the FDTD lattice.

It is the relationship among the electric field E, the displacement D, and the polarizations P, which defines the type of material being simulated. Optical fibers often display dispersive characteristics necessitating the linear polarization. In order to simulate high-intensity laser light, it is necessary to include the nonlinear polarization. The implementation of complex linear and nonlinear polarizations into FDTD has been described elsewhere [7], [8]. Two of the simpler examples will be reviewed briefly.

A. Formulation of the Nonlinear Polarization

The nonlinear polarization is formulated as an intensity-dependent refractive index, i.e., the Kerr effect

$$P_{\mathrm{NL}}(t) = \chi^{(3)} E^3(t). \tag{3}$$

Start by taking a Taylor series expansion of $E^3(t)$ around the point $t = t_{n-1}$ and evaluating it at the point $t = t_n$

$$\begin{aligned} E^3(t_n) &= E^3(t_{n-1}) + \frac{d}{dt}\left(E^3(t_{n-1})\right)(t_n - t_{n-1}) \\ &= 3 \cdot E^2(t_{n-1}) \cdot E(t_n) - 2 \cdot E^3(t_{n-1}). \end{aligned} \tag{4}$$

Naturally, it will be assumed that the times t_{n-1} and t_n correspond to times in the FDTD formulation, thus, (4) will be written

$$(E^n)^3 \cong 3 \cdot (E^{n-1})^2 \cdot (E^n) - 2 \cdot (E^{n-1})^3.$$

Finally, substituting this approximation for $(E^n)^3$ into (3), E^n can be determined by

$$E^n = \frac{D^n + \chi_0^{(3)} 2 \cdot (E^{n-1})^3}{\varepsilon_r + \chi_0^{(3)} 3 \cdot (E^{n-1})^2}. \tag{5}$$

Note that the new value of $E(t)$, E^n, is calculated from the new value of $D(t)$, D^n, and previous values of $E^2(t)$ and $E^3(t)$, i.e., $(E^{n-1})^2$ and $(E^{n-1})^3$.

B. Formulation of the Linear Polarization $P_L(t)$

The linear polarization of (1b) is

$$P_L(t) = \varepsilon_0 \int_0^t \chi^{(1)}(t-\tau) \cdot E(\tau)\, d\tau. \tag{6}$$

$\chi^{(1)}$ is a second-order Lorentz linear dispersion, usually described in the frequency domain as

$$\chi^{(1)}(\omega) = \frac{\varepsilon_s - \varepsilon_\infty}{1 + j2\delta_L(\omega/\omega_L) - (\omega/\omega_L)^2}. \tag{7}$$

Taking the Z transform of (6) and (7) gives [7], [8]

$$\begin{aligned} P_L(z) &= \varepsilon_0 \chi^{(1)}(z) \cdot E(z) \cdot \Delta t \\ &= \varepsilon_0 \frac{\gamma_L \cdot \Delta t \cdot e^{-\alpha_L \cdot \Delta t} \cdot \sin(\beta_L \cdot \Delta t) \cdot z^{-1}}{1 - 2 \cdot e^{-\alpha_L \Delta t} \cdot \cos(\beta_L \cdot \Delta t) \cdot z^{-1} + e^{-2\alpha_L \Delta t} \cdot z^{-2}} \\ &\quad \cdot E(z) \end{aligned}$$

where

$$\begin{aligned} \alpha_L &= \omega_L \cdot \delta_L \\ \beta_L &= \omega_L \cdot \sqrt{1 - \delta_L^2} \\ \gamma_L &= \frac{\omega_L \cdot (\varepsilon_s - \varepsilon_\infty)}{\sqrt{1 - \delta_L^2}}. \end{aligned}$$

Defining the new variable

$$S_L(z) = \frac{z P_L(z)}{\varepsilon_0}$$

and moving to the sampled time domain, E is determined by

$$E^n = D^n - S^{n-1} \tag{8a}$$

$$S_L^n = c1 \cdot S_L^{n-1} - c2 \cdot S_L^{n-2} + c3 \cdot E^n \tag{8b}$$

where

$$\begin{aligned} c1 &= 2 \cdot e^{-\alpha_L \cdot \Delta t} \cdot \cos(\beta_L \cdot \Delta t) \\ c2 &= e^{-2\alpha_L \cdot \Delta t} \\ c3 &= \gamma_L \cdot \Delta t \cdot e^{-\alpha_L \cdot \Delta t} \cdot \sin(\beta_L \cdot \Delta t). \end{aligned}$$

Combining this with the nonlinear polarization, the E-field calculation now consists of

$$E^n = \frac{D^n + \chi_0^{(3)} 2 \cdot (E^{n-1})^3 - S_L^{n-1}}{\varepsilon_r + \chi_0^{(3)} 3 \cdot (E^{n-1})^2} \tag{9a}$$

and

$$S_L^n = c1 \cdot S_L^{n-1} - c2 \cdot S_L^{n-2} + c3 \cdot E^n. \tag{9b}$$

Verification of the accuracy of these formulations has been described in [7]–[9].

III. Simulation of a Three-Dimensional Optical Fiber

This section describes the simulation of single-mode polymer optical fibers [10]. The three-dimensional simulation of an optical fiber via the FDTD method has some substantial logistical problems stemming from the fact that light pulses consist of very high-frequency EM energy. The high frequency means very small wavelengths. As an example, an Nd : YAG laser produces light with a wavelength of 1.064 μm. The dielectric constant being used is 2.19, thus, the wavelength in the fiber is actually 0.72 μm. To accurately calculate phase shifts over long distances, it is desirable to have 30 points per wavelength [11], giving a cell size of 0.024 μm. A typical single-mode fiber might have a core of 10 μm in diameter. It is not necessary to model the entire cladding, but about 7 μm on each side is needed. A 10 μm length of fiber results in a volume of 24 μm $\times$ 24 μm $\times$ 10 μm, which requires a problem space of $1000 \times 1000 \times 400 = 400$ million cells. This would overwhelm even today's supercomputers.

Sections III-A-D discuss what can be done to make the simulation of an optical fiber a tractable problem.

A. Initializing in the Propagation Mode

When a laser pulse impinges on an optical fiber, it can take a certain amount of time for the pulse to settle into one or more of the propagating modes of the fiber. This may only be a centimeter, but we cannot afford to model such a length while waiting to establish the propagation mode. Therefore, it is necessary that the incident wave be a propagating mode. This is done by determining the relative amplitude distribution of the E-field at the incident plane. In single-mode propagation of a step-indexed fiber, the amplitude profile of the predominant electric field may be written as the Gaussian function [12]

$$\phi = e^{-r^2/\omega_0^2} \tag{10}$$

where r is the distance from the middle of the fiber and ω_0 is the "spot size" or radius of the fundamental mode. The spot size is calculated from

$$\omega_0 = (0.65 + 1.619 \cdot V^{-3/2} + 2.879 \cdot V^{-6}) \cdot a$$

where a is the radius of the core of the fiber and V is the normalized frequency, which is calculated from

$$V = \frac{2\pi}{\lambda} a \cdot (\varepsilon_{\text{core}} - \varepsilon_{\text{cladding}}).$$

The free-space wavelength of the light is λ, and $\varepsilon_{\text{core}}$ and $\varepsilon_{\text{cladding}}$ are the dielectric constants of the core and cladding.

B. Oblong Cells

To minimize the effects of dispersion, it is desirable to have as many points per wavelength as possible in the direction of propagation [11]. We have chosen 30 points per wavelength. However, the shape of the pulse in the transverse directions changes relatively slowly. Therefore, we are using cells which are 0.023 μm in the direction of propagation and 0.138 μm in the transverse direction, i.e., one-sixth as large in the propagation direction as the transverse. This gives the desired accuracy in the direction of propagation where the shape is changing rapidly, but minimizes the number of cells in the transverse direction.

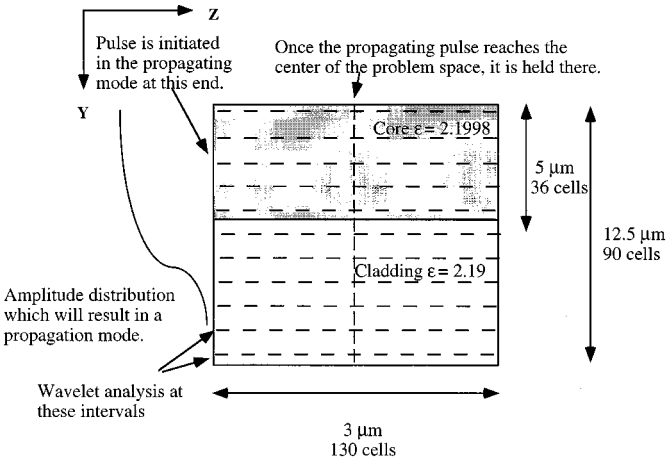

Fig. 1. Diagram of the problem space for the FDTD simulation. A propagating mode pulse is activated on the left-hand side. The E-field is polarized in the X-direction. Any time the pulse reaches the middle, all fields are shifted back one cell, having the effect of holding the pulse in the middle of the problem space. A wavelet analysis is done in the propagation direction at intervals of ten cells in the transverse direction.

C. Use of Twofold Symmetry of the Transverse Field

The optical fibers we are simulating use single-mode propagation [13]. The four quadrants in the transverse field are symmetric about their axes [12]. This symmetry can be exploited by simulating only one quadrant in the FDTD simulation. Fig. 1 is a diagram of the problem space used in the FDTD simulation. The core has a 5-μm radius with a dielectric constant of 2.1998 versus 2.19 in the cladding. Notice that 7.2 μm of cladding is simulated, which is adequate for the pulse to die out in the transverse direction. It is important that the pulse die out completely to avoid "waveguiding" on the edge of the problem space.

D. Moving Problem Space

As the pulse is propagating down the fiber, the mean position is being calculated on the axis in the center of the core

$$\text{Position} = \frac{\sum_{j=1}^{j\max} j \cdot E^2(j)}{E_{\text{Total}}} \tag{11}$$

where

$$E_{\text{Total}} = \sum_{j=1}^{j\max} E^2(j).$$

(This is recognizable as the "expectation of the position" from quantum mechanics.) When the value of *Position* reaches one-half the length of the buffer, the program stops and moves every E- and H-field values back one cell in the propagating

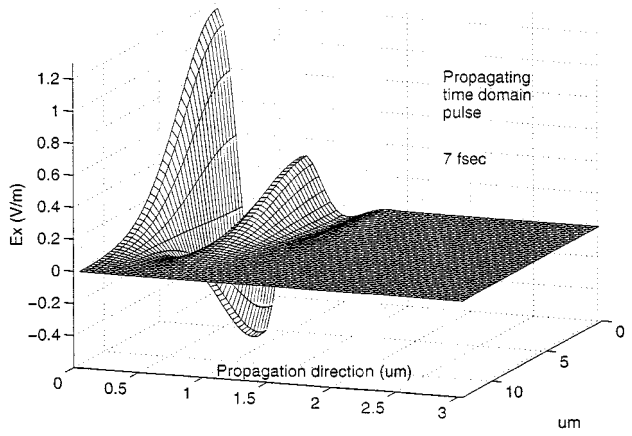

(a)

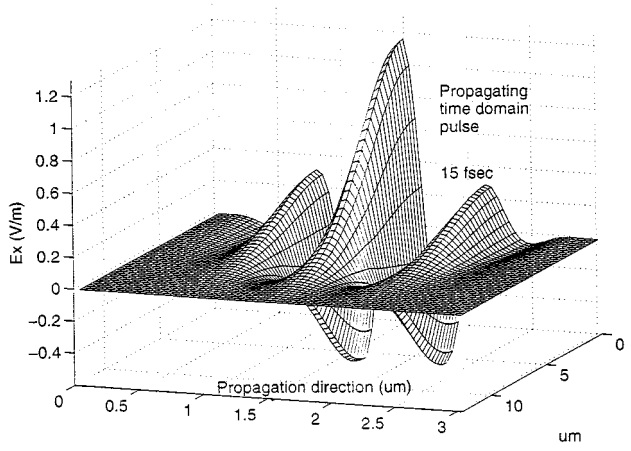

(b)

Fig. 2. Time-domain propagating pulse. The pulse is a cosine function in a Gaussian envelope of 10 fs. It is initiated on the left-hand side (a) and propagates until it reached the middle of the problem space (b).

direction. The simulation is continued until *Position* again reaches the halfway point, and the process is repeated. This has the effect of holding the pulse in the middle of the problem space.

Fig. 2 shows a simulation of a pulse propagating in the problem space of Fig. 1. It uses the symmetries described above and the oblong cells. Fig. 2(a) shows the pulse after 7 fs. It was initiated in the propagating mode from the left-hand side. The pulse is a cosine function at 282 THz inside a Gaussian envelope of 10 fs. Each time step is .038 fs. After 15 fs [see Fig. 2(b)], it has reached the center of the problem space and will remain in this position relative to the total problem space. However, it may substantially change in amplitude and shape as it propagates along the fiber.

IV. Analysis of the Pulse

Even though the pulse is being held in the middle of the problem space, its characteristics are being analyzed to determine what changes are taking place as it propagates. This analysis is in two parts: a Fourier transform to determine the macroscopic properties of amplitude and phase and a wavelet decomposition to record the shape of the pulse in the transverse and propagating directions.

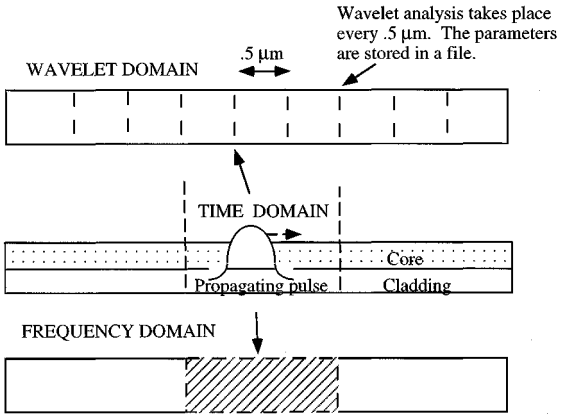

Fig. 3. Time-domain problem space is assumed to be moving along a fiber. The discrete Fourier transform is being calculated and mapped to another domain. At the same time, wavelet analysis is done at 0.5-μm intervals and the parameters stored.

Fourier Transform: While the time-domain pulse is being simulated, the Fourier transform of the pulse throughout the problem space is being calculated at the center frequency of 282 THz. This is done through a "running Fourier transform," which allows the Fourier transform to be calculated while the time-domain program is running [14]. However, the results of this Fourier transform are mapped to a unique position in the propagating direction that allows for the moving problem space (Fig. 3). In this manner, the amplitude and phase of the propagating pulse can be calculated over distances much larger than the section of fiber being simulated.

Fig. 4(a) shows the resulting Fourier amplitude of the fiber in Fig. 1 from a simulation carried out over a length of 10 μm. The amplitude is displayed for the YZ-plane, the Z-direction being the direction of propagation; the E-field is polarized in the X-direction. Notice that the profile has retained the Gaussian shape, indicating that it has maintained a propagating mode. Fig. 4(b) displays the phase along the center axis in the direction of propagation. (A two-dimensional display of the phase is difficult to interpret.) Fig. 4(b) is actually the phase difference between the phase of the propagating pulse, and the phase of a plane wave propagating in a medium of cladding. (This is being calculated by a one-dimensional FDTD simulation that takes place simultaneously.) The linearly decreasing phase if Fig. 4(b) means that the pulse propagating in the core is lagging behind the plane-wave pulse in the cladding, which is to be expected.

A quantity of interest is the amount of phase shift that is induced in a nonlinear material compared to the linear [2], [13]. The simulation is repeated for the same fiber with a nonlinearity of $\chi^{(3)} = 10^{-7}$. The Fourier amplitude profile for the nonlinear simulation is indistinguishable from Fig. 4(a). However, the phase down the center axis of the pulse is different for the nonlinear case (Fig. 5). The phase difference between nonlinear and linear increases steadily with distance, as it should. Over this short distance of 10 μm, there is a phase difference of 0.00012°. Researchers doing interferometric experiments are

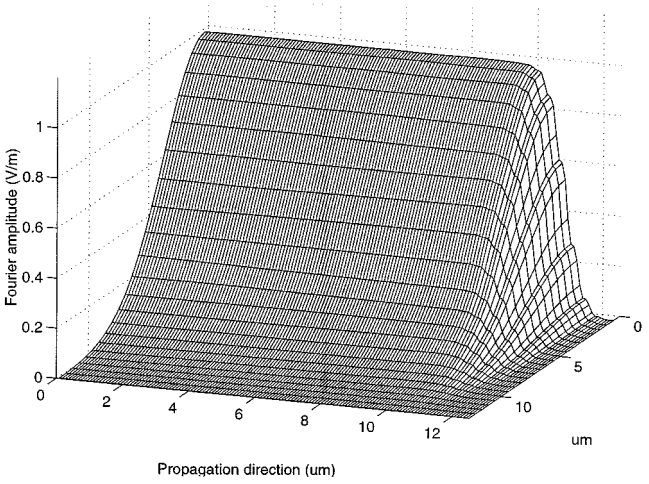

(a)

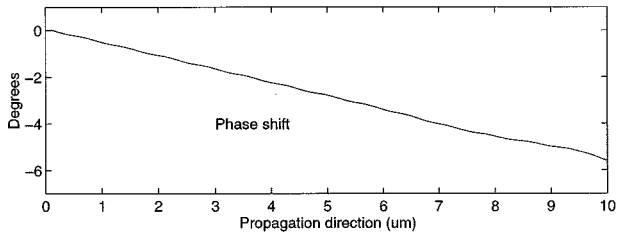

(b)

Fig. 4. Fourier analysis of a pulse which has propagated 10 μm. The amplitude (a) is a two-dimensional plot in the YZ-plane. The solid Gaussian shape of the amplitude indicates that the pulse remained in the propagating mode. The phase (b) is only displayed along the center propagation axis. The phase is actually the difference between the phase of the propagating pulse in the fiber and the phase of a plane wave propagating in cladding material.

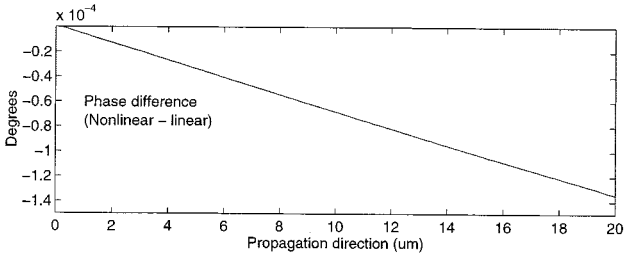

Fig. 5. Phase difference between a nonlinear fiber with $x^{(3)} = 10^{-7}$ and the linear fiber of Fig. 4.

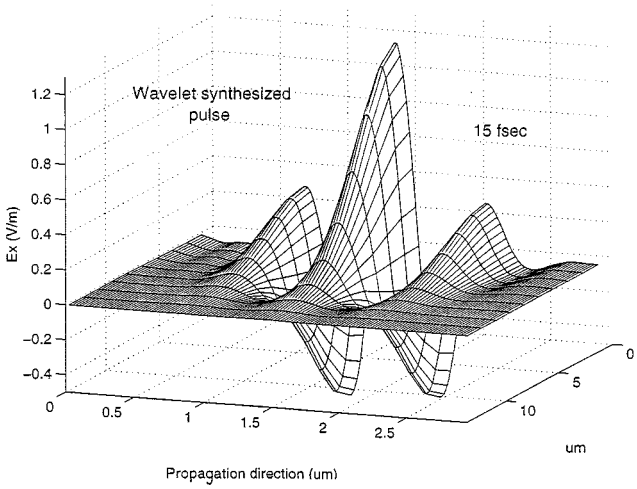

Fig. 6. Wavelet synthesis of the pulse in Fig. 2.

interested in the distance it takes to obtain a phase shift of 180°. Based on the results of Fig. 5, it would require a distance of

$$\frac{20\ \mu\text{m}}{0.00012^\circ} \times 180^\circ = 30\ \text{m}. \tag{12}$$

In a typical interferometric experiment, like those with a Sagnac interferometer [13], a pulse is sent in two different directions through a section of nonlinear optical fiber. In one direction, the pulse has a large enough amplitude to induce the nonlinearity; in the other direction, it does not. At the end, the pulses are recombined. The larger pulse sees a different index of refraction caused by the nonlinearity and, therefore, travels at a different speed. If enough phase shift between the two is induced, this results in destructive interference, and the pulse propagates no further. Therefore, the change in phase between linear and nonlinear is the crucial parameter. Equation (12) agrees qualitatively with the experimental results of Garvey *et al.* [13].

Wavelet Analysis: As the simulation is progressing, a wavelet analysis of the propagating pulse takes place every 0.5 μm (Fig. 1). The wavelet analysis allows the shape to be stored with a minimum number of variables, which means relatively long distances can be simulated without using excessive storage. The ability to analyze the shape of the pulse is important because Fourier analysis alone does not necessarily document distortions that the pulse may have undergone.

The wavelet analysis is done with a fifth-order fast wavelet transform. The filters are a biorthogonal 9/7 pair [15]. The 130 cells in the direction of propagation can be represented by only 16 parameters after analysis.

The analysis is done on a two-dimensional cut of the propagating pulse in the YZ-plane, as shown in Fig. 1. It is not necessary to do three-dimensional analysis because of the symmetry in the other transverse direction. The wavelet analysis is done in the propagating direction only at intervals of ten cells in the transverse direction. The data is stored as the analysis is made, and then the pulse can be synthesized later. Synthesis in only done in the propagation direction, with simple averaging in the transverse direction. Fig. 6 was synthesized from the analysis of the pulse in Fig. 2. However, the pulse in Fig. 2 required $90 \times 130 = 11700$ values. The synthesized pulse required $9 \times 16 = 144$ parameters.

A simulation of a fiber similar to those described above was made, except that the second-order Lorentz dispersion described in Section II was added. The characteristics were $\chi^{(1)} = 0.05$, $\omega_L = 140$ THz, and $\delta = 0.000025$. Fig. 7 shows the pulse at various times during the propagation as synthesized from the wavelet parameters. The dispersion has resulted in substantial distortion of the pulse as it propagates. This is not information that would be available from Fourier analysis. In fact, the Fourier amplitude is almost indistinguishable from Fig. 4(a). This type of change is significant when propagation over long distances is desirable.

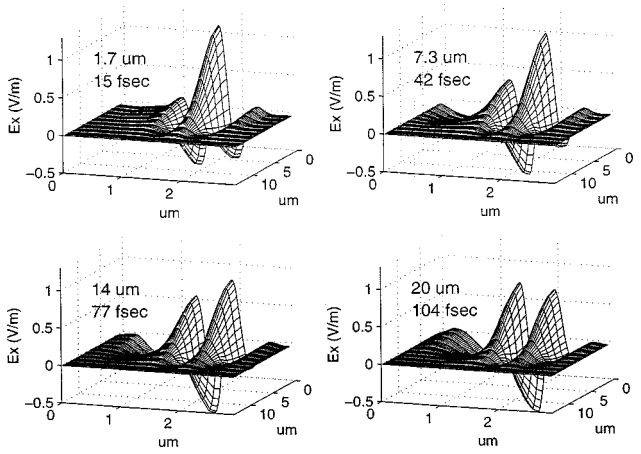

Fig. 7. Wavelet synthesis of the propagating pulse at various points along a dispersive fiber.

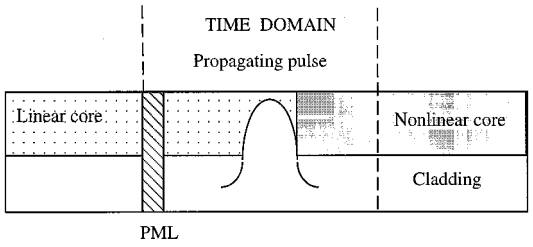

Fig. 8. Time-domain problem space is assumed to be moving along a fiber as before. After the pulse has propagated past the first five cells, a PML is activated. A nonlinear core is moved into the problem space after the pulse has traveled 5 μm.

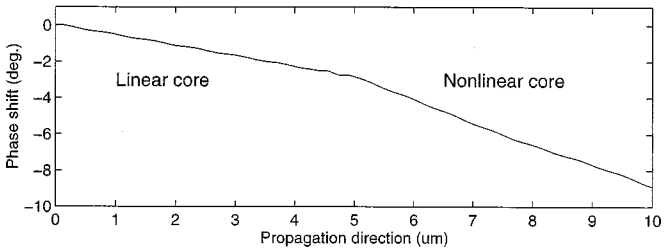

Fig. 9. Phase of the pulse, which begins propagating in a linear fiber and encounters a nonlinear fiber with $\chi^{(3)} = 10^{-2}$ after 5 μm.

V. Simulation of a Change in the Fiber

As a final example, the simulation of a pulse encountering a new core material will be described. Specifically, we simulate a propagating pulse in a linear fiber that suddenly encounters a nonlinear fiber. This is illustrated in Fig. 8, where a different core is moved into the problem space. The first part of the fiber is the same as that used in Section III, i.e., the core is $\varepsilon_{\text{core}} = 2.1998$ with a cladding of $\varepsilon_{\text{cladding}} = 2.19$. At 5 μm, it encounters a nonlinearity of $\chi^{(3)} = .01$ (this is an unrealistically large nonlinearity that is used for illustrative purposes). Since there is a transition from one type of material to another, one part of the pulse will be transmitted into the new material, and another part will be reflected. While the vast majority of the energy will be transmitted in this case, some will be reflected. This necessitates an absorbing boundary condition to keep the scattered wave from being reflected back into the problem space. This is accomplished by a perfectly matched layer (PML) [16], which is implemented in the first five cells in the propagation direction, but which is only activated after the propagating wave has completely passed. (Fig. 8). If the scattering were more substantial, it would also have to be activated on the sides, but this is probably not necessary for the present problem.

This new nonlinearity does not substantially affect the Fourier amplitude or the time-domain pulse shape. However, as we saw in the previous section, the nonlinearity does affect the phase. Fig. 9 shows the results. At 5 μm, the rate of phase shift almost doubles. Obviously, the same technique could be used to change the dielectric constant, to add a linear polarization, or even to change the size of the core.

VI. Summary

In this paper, we have described techniques for a true three-dimensional simulation of an optical fiber using the FDTD method. This was accomplished partly by exploiting the symmetry of the single-mode optical fiber and by using oblong cells to obtain high resolution in the propagating direction. However, most significant was the use of a moving problem space, which limited the size of the actual time-domain calculation, but could simulate a pulse over relatively long distances. Fourier and wavelet analysis were used to calculate important parameters and characterize the pulse shape.

The programs described in Sections IV and V required 13.4 megawords of core memory in a Cray T90 supercomputer. The simulation of a 20-μm section of fiber requires 400 central processing unit (CPU) s. Simulations like this require state-of-the-art computer resources, but not extraordinary resources. They could easily be run on a high-end work station.

Although this paper focused on the simulation of optical fibers, some or all of these techniques could be used to simulate a pulse propagating in any electrically long object such as a dielectric waveguide.

References

[1] A. Taflove, *Computational Electrodynamics: The Finite-Difference Time-Domain*. Norwood, MA: Artech House, 1995.

[2] M. Jinno and T. Matsumoto, "Ultrafast all-optical logic operations in a nonlinear Sagnac interferometer with two control beams," *Opt. Lett.*, vol. 16, pp. 220–222, Feb. 1991.

[3] M. B. Kuzyk, U. C. Paek, and C. W. Dirk, "Guest host polymers for nonlinear optics," *Opt. Lett.*, vol. 16, pp. 902–904, Aug. 1991.

[4] P. M. Goorjian and A. Taflove, "Direct time integration of Maxwell's equations in nonlinear dispersive media for propagation and scattering of femtosecond electromagnetic solitons," *Opt. Lett.*, vol. 17, pp. 180–182, Feb. 1992.

[5] R. M. Joseph, P. M. Goorjian, and A. Taflove, "Direct time integration of Maxwell's equations in two-dimensional dielectric waveguides for propagation and scattering of femtosecond electromagnetic solitons," *Opt. Lett.*, vol. 18, pp. 491–493, April 1992.

[6] K. S. Yee, "Numerical solution of initial boundary value problems involving Maxwell's equations in isotropic media," *IEEE Trans. Antennas Propagat.*, vol. AP-14, pp. 585–589, Apr. 1966.

[7] D. M. Sullivan, "Nonlinear FDTD formulations using Z transforms," *IEEE Trans. Microwave Theory Tech.*, vol. 43, pp. 676–682, Mar. 1995.

[8] D. M. Sullivan, "Z transform theory and the FDTD method," *IEEE Trans. Antennas Propagat.*, vol. 44, pp. 28–34, Jan. 1996.

[9] D. M. Sullivan and M. Kuzyk, "Three dimensional nonlinear optical fiber simulation," in *4th Int. Millimeter Submillimeter Waves Applicat. Conf.*, San Diego, CA, July 20–24, 1998, pp. 1325–1329.
[10] D. W. Garvery, K. Zimmerman, P. Young, J. S. Townsend, Z. Zhou, M. Lobel, M. Dayton, W. Wittorf, and M. G. Kuzyk, "Single-mode nonlinear-optical polymer fibers," *J. Opt. Soc. Amer. B., Opt. Phys.*, vol. 13, pp. 2017–2023, Sept. 1996.
[11] K. L. Shlager, J. G. Maloney, S. L. Ray, and A. F. Peterson, "Relative accuracy of several finite-difference time-domain methods in two and three dimensions," *IEEE Trans. Antennas Propagat.*, vol. 41, pp. 1732–1737, Dec. 1993.
[12] J. Senior, *Optical Fiber Communications*. Englewood Cliffs, NJ: Prentice-Hall, 1985.
[13] D. W. Garvery, Q. Li, M. G. Kuzyk, C. W. Dirk, and S. Martinez, "Sagnac interferometric intensity-dependent refractive-index measurements of polymer optical fiber," *Opt. Lett.*, vol. 21, pp. 104–106, Jan. 1996.
[14] D. M. Sullivan, "Mathematical methods for treatment planning in deep, regional hyperthermia," *IEEE Trans. Microwave Theory Tech.*, vol. 30, pp. 864–872, May 1991.
[15] G. Strang and T. Nguyen, *Wavelets and Filter Banks*. Wellesley, MA: Wellesley-Cambridge, 1996.
[16] D. M. Sullivan, "An unsplit step 3-D PML for use with the FDTD method," *IEEE Microwave Guided Wave Lett.*, vol. 7, pp. 184–186, July 1997.

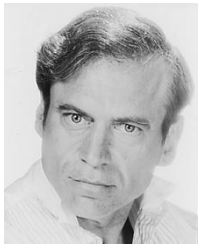

Dennis Sullivan (M'89–SM'95) received the Ph.D. degree in electrical engineering from the University of Utah, Salt Lake City, in 1987.

From 1987 to 1993, he was a Research Engineer at the Stanford University School of Medicine, where he developed a treatment planning system for hyperthermia cancer therapy. He is currently an Associate Professor of electrical engineering at the University of Idaho, Moscow. His current research interests include nonlinear optical simulation and semiconductor quantum simulation.

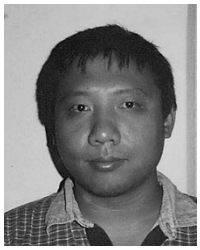

Jun Liu was born in Beijing, China. He received the B.S. degree in microwave engineering from Beijing Broadcasting Institute, Beijing, China, in 1994, and the M.S. degree in electrical engineering from the University of Idaho, Moscow, in 1999.

He is currently a Test Engineer with Maxim Integrated, Portland, OR.

Mark Kuzyk received the B.S., M.S., and Ph.D. degrees from the University of Pennsylvania, Philadelphia, in 1979, 1981, and 1985, respectively, all in physics. His graduate work focused on nonlinear optics of organic liquids.

From 1985 to 1990, he was involved with dye-doped polymeric nonlinear optical materials at AT&T Bell Laboratories as a Member of the Technical Staff. In 1990, he accepted a faculty position in physics at Washington State University, Pullman, where he has been involved with nonlinear optics in fibers and fiber-based devices. He is currently an Associate Professor of physics and Chair of the Materials Science Program. He has over authored or co-authored 100 publications and *Characterization Techniques and Tabulations of Organic Nonlinear Optical Materials* (New York: Marcel Dekker, 1998). He holds several patents. He is an Editor of the *Journal of the Optical Society B—Optical Physics*.

Dr. Kuzyk is a Fellow of the Optical Society of America (OSA) and a member of the American Physical Society and The International Society for Optical Engineers (SPIE).